

Optical Modes in Semiconductor Microtube Ring Resonators

T. Kipp,* H. Welsch, Ch. Strelow, Ch. Heyn, and D. Heitmann

Institut für Angewandte Physik und Zentrum für Mikrostrukturforschung, Universität Hamburg, Jungiusstraße 11, 20355 Hamburg, Germany

(Received 31 October 2005; published 24 February 2006)

We demonstrate optical modes in InGaAs/GaAs microtubes acting as optical ring resonators. Self-supporting microtubes were fabricated by optical lithography and wet-etching processes utilizing the self-rolling mechanism of strained bilayers. The optical modes were probed by the photoluminescence of InAs quantum dots embedded in the tube's wall. In this novel microtube ring resonator we find a spectrum of sharp modes. They are in very good agreement with the theoretical results for a closed thin dielectric waveguide.

DOI: [10.1103/PhysRevLett.96.077403](https://doi.org/10.1103/PhysRevLett.96.077403)

PACS numbers: 78.66.Fd, 42.55.Sa, 42.82.Cr, 81.16.Dn

Semiconductor microcavities containing quantum dots (QDs) or quantum wells have gained considerable interest in the past years, both for fundamental research on light-matter interaction and for applications like low-threshold lasers. Examples for lithographically structured semiconductor microcavities are microdisks [1], micropillars [2], and photonic-crystal microcavities [3]. In all these structures low-threshold lasing has been achieved and cavity quantum electrodynamic (CQED) effects of zero-dimensional electron systems interacting with optical modes, like the Purcell effect or Rabi splitting, have been observed [4–7]. In the cases mentioned above the optically active systems, i.e., the QDs, originate by self assembly, whereas the resonators were manufactured following a pure top-down approach.

By using the self-rolling mechanism of a thin pseudo-morphically strained semiconductor bilayer it is possible to fabricate three-dimensional objects—like lamellas or tubes—out of two-dimensional epitaxial layers [8,9]. The roll diameter, ranging between some nanometers and several hundred microns, can be precisely controlled by varying the incorporated strain of the bilayer [10,11]. Length, position, and number of tube walls can be controlled by standard semiconductor lithography techniques [12–14]. In the field of optics, self-rolling strained bilayers have been used to fabricate micromirrors with electrostatic actuation [15]. Furthermore, the photoluminescence of strained thin quantum wells has been studied [16].

In this work we demonstrate that the self-assembling process of strain relaxation in a InGaAs/GaAs bilayer can be used to fabricate cylindrical micron-sized optical ring resonators. To probe their mode structure, we incorporated a luminescent material as an internal light source in the ring cavity, namely, self-assembled InAs QDs [2]. It is an intrinsic property of a microtube ring resonator that the embedded optically active material is located close to the maximum optical field intensity. Sharp polarized and regular optical modes are observed with a mode spacing of about 18 meV, being consistent with a theoretical modeling. We proof the striking homogeneity of the microtube resonator, raising the hope for future application of this

novel kind of microcavity in optoelectronic devices or CQED experiments.

The starting point for the fabrication of our microtube bridges is a molecular-beam epitaxy (MBE)-grown sample [Fig. 1(a)]. On top of the GaAs substrate and a buffer layer, 40 nm AlAs serves as a sacrificial layer in the later lift-off process, whereas 20 nm epitaxially grown $\text{In}_{0.2}\text{Ga}_{0.8}\text{As}$, together with the following 30 nm-layer GaAs, form the strained bilayer. In the middle of the top GaAs layer, i.e., just 15 nm beneath the sample surface, one layer of self-

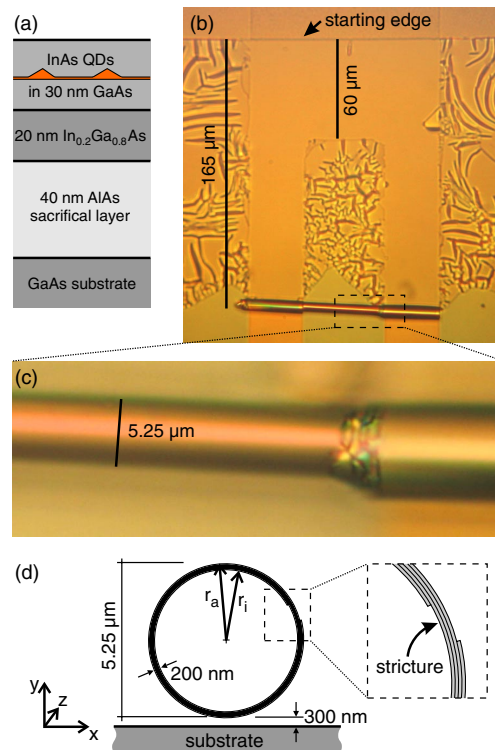


FIG. 1 (color online). (a) Schematic sample structure. (b) Optical microscope image of a microtube bridge. The U-shaped part has a rolled-up beginning at the starting edge. (c) High resolution optical microscope image of the microtube bridge and its bearing. (d) Scaled schematic section of the self-supported part of the microtube.

assembled InAs QDs is grown. The lithographic preparation resembles in some ways the ones in our previous work [13,14], but the challenge here is to separate the microtube from the substrate to avoid radiative losses. We start with the definition of a U-shaped [see Fig. 1(b)] strained mesa by a shallow wet-chemical etching into the $\text{In}_{0.2}\text{Ga}_{0.8}\text{As}$ layer using a $\text{H}_2\text{O}_2/\text{H}_3\text{PO}_4$ solution. Then we define the starting edge by deep etching through the AlAs sacrificial layer, where, in the last step, the highly-selective HF solution starts to undercut the strained $\text{In}_{0.2}\text{Ga}_{0.8}\text{As}$ layer. Over the full width of the strained mesa the self-rolling mechanism starts and multiwalled microtubes are formed. After a distinct distance defined by the U-shaped mesa, (60 μm for the tube shown in Fig. 1), only the side pieces of the tube continue rolling. This raises the center tube, leading to a self-supporting microtube “bridge,” where in the middle part the tube is separated from the substrate [see Fig. 1(c)]. We fabricated several microtubes with different mesa dimensions with similar experimental findings. In the following, we will concentrate on our results for the microtube depicted in Fig. 1. The actual microtube bridge has an overall length of 120 μm with bearings of 35 μm on each side. The roll-up length of the self-supporting part is 60 μm , its outer diameter is measured to be 5.25 μm . Taking into account the spiral shape of the tube this leads to a number of revolutions of about 3.8. The inner radius of about 2.4 μm agrees well with the calculated value using the formula of Tsui and Clyne [17]. The side pieces of the microtube forming the bearings of the bridge have rolled over a length of about 165 μm , corresponding to about 10 revolutions. This leads to a lifting of the actual microtube of approximately 0.3 μm above the substrate.

The optical properties of the microtubes were investigated by microphotoluminescence (PL) spectroscopy. The sample was mounted in an optical continuous-flow cryostat and cooled to $T = 5$ K. The exciting He-Ne laser ($\lambda = 633$ nm) was focused onto the sample by a microscope objective ($\times 80$, 0.75 NA). The emitted light was collected by the same objective and then spectrally analyzed by a triple-grating spectrometer and detected by a Peltier-cooled deep-depletion CCD camera.

Figure 2 shows PL spectra of the microtube for the different polarization configurations. The striking feature of this spectrum is the regular sequence of sharp peaks superimposed on a broad background from the luminescence of the QDs. These sharp peaks correspond to linear polarized light with its electric field vector parallel to the tube axis ($\vec{E} \parallel \vec{z}$). We refer to this as the transverse electric (TE) polarization. The peaks do also appear in the TM polarized spectrum, but only with a fraction of intensity. This results from crosstalk due to the finite polarization selectivity of our micro-PL setup. In the following we first will work out that these peaks are optical resonances arising from constructive interference of light with itself, proving the microtube bridge to be an optical ring resona-

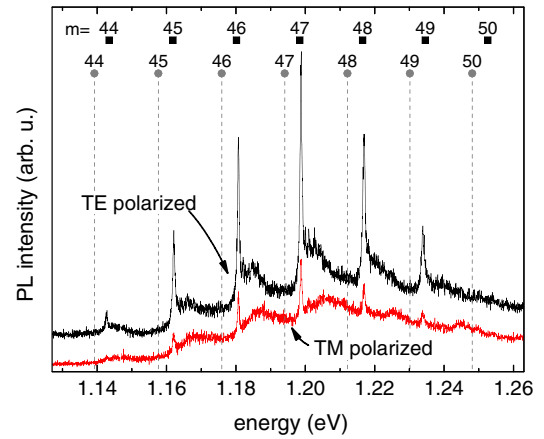


FIG. 2 (color online). Micro-PL spectra of a microtube bridge measured in TE (upper graph) and TM (lower graph) polarization configuration. The spectra are vertically shifted for clarity. The symbols indicate calculated mode positions (without any fitting) labeled with their azimuthal mode number m . The squares (circles) represent the waveguide (exact) approach.

tor. First of all, the peaks do not appear in spectra of the unstructured sample (not shown). Thus the peaks are not characteristic for the QDs but originate from the microtube. Secondly, sharp peaks do also not appear in spectra of microtubes lying on the substrate. The spectra measured on the side pieces of the microtube (not shown) exhibit only weak and broad features with a smaller spacing. The different spacing is consistent with a larger outer radius of the tube. The broadness can be explained by the shorter photon lifetime due to strong losses into the substrate. Third, scanning the exciting laser over different positions of the microtube perpendicular to the tube axis leads to spectra, in which the peak positions do not change. This is what one would expect, when the peaks arise from photons running in circles around the tube axis.

To compare our spectrum to the theory, we regard the microtube as a planar dielectric waveguide (with refractive index n) surrounded by air and apply periodic boundary conditions for the propagation of light in the waveguide. The height of the waveguide is chosen to be $h = (r_a - r_i)$, i.e., the tube wall thickness [see Fig. 1(d)]. We first calculate the modes of the planar waveguide and assign them to an effective refractive index n_{eff} [18]. The periodic boundary condition $n_{\text{eff}}l = \lambda m$, with the tube circumference $l = 2\pi(r_a - h/2)$, the vacuum wavelength of the propagating light λ , and the azimuthal mode number $m \in \mathbb{N}$, then ensures that in case of resonance, the light has the same phase after a round trip. The modes in Fig. 2 are polarized parallel to the tube axis corresponding to TE modes in the waveguide description. Averaging spatially over the bilayer, we assume an energy-dependent refractive index of $n(E) = 3.46 + (E[\text{eV}] - 1.1)/2$ [19,20]. Note, that it is important to include the energy dependence of the refractive index, which varies significantly close to the band edge of the semiconductor. Calculating with $h = 200$ nm and

$2r_a = 5.25 \mu\text{m}$ leads for the lowest lying TE mode perpendicular to the waveguide to mode positions as depicted in Fig. 2 by squares. The modes are labeled by their azimuthal mode number m . These calculated values seem to fit nearly perfectly to the measurements. One has to keep in mind that the mode position is very sensitive to the radius of the microtube. For example, a change in radius of 50 nm leads to a shift of about 15–19 meV. Since the radius is only measured from the microscope picture, the exact position of the calculated modes are afflicted with some uncertainty. More importantly, the mode spacing is in very good agreement with the measurements. In a second theoretical approach, we try to find the exact solutions for a dielectric disk with a hole in its center. Starting from Maxwell's equations, one sets up a Schrödinger-like wave equation and solves the eigenvalue problem using the boundary conditions known from Maxwell's equations [21]. The dots in Fig. 2 represent the results obtained from this solution. The deviation to our first approach is very small. Especially the mode spacings fit perfectly. This shows that the first approach, which is easier to calculate, delivers sufficient accurate results.

Using again the waveguide approach, a waveguide height of $h = 200 \text{ nm}$ would allow also the TM ground mode and the second TE mode to propagate. Therefore one would expect to measure two further sets of modes. We first consider the TE case. Beside the sharp modes identified with the ground mode family we observe on the high-energy side of each mode a broader signal, sometimes superimposed with a fine structure. These broader signals are regular with the peaks of the first TE family and therefore cannot be attributed to the second TE family, for which a smaller mode spacing is calculated. The absence of the second TE family can be explained remembering that the number of revolutions of the microtube is about 3.8. This means that the tube wall thickness is not constant but has a stricture [see Fig. 1(d)], where the thickness changes from 200 to 150 nm. We calculate that for a 150 nm waveguide the second TE mode does not exist. Therefore the narrowing inhibits the development of second order TE modes. In the TM polarization configuration, no evident optical modes are observed, although they should theoretically exist in waveguides with heights down to about 60 nm. The reason of this behavior might again be the constriction. Altering the waveguide height from 200 to 150 nm changes n_{eff} from 2.52 to 1.72 (assuming $E = 1.2 \text{ eV}$). This jump is much steeper compared to the TE case (3.07 and 2.87). A small n_{eff} is equivalent to a less confined field. On the other hand, a less confined field is more susceptible to imperfections of the waveguide surfaces, especially to the abrupt changes of the tube wall thickness at both sides of the stricture. These imperfection may lead to scattering losses and therefore to a broadening of the modes.

The results reported so far clearly demonstrate that the resonances are indeed optical modes of the microtube,

which are observed here for the first time. Within the remaining space we would like to discuss some further interesting details. Figure 3(a) shows TE spectra obtained for different positions of the exciting laser on the microtube axis. Here, $z = 0$ is somewhere in the middle of the self-supporting tube. The distance between two adjacent positions on the sample is less than $1 \mu\text{m}$. The PL intensity is encoded in a gray scale, where dark means high intensity. In the displayed energy range each spectrum exhibits two groups of peaks representing two optical modes with neighboring azimuthal mode numbers m . Over a distance of about $20 \mu\text{m}$ along the microtube, the optical mode positions shift less than 2 meV. A shift in radius of the microtube of just 0.3% would lead to a larger shift. This impressively demonstrates the homogeneity of the microtube and of its underlying self-rolling mechanism. Figure 3(b) shows the spectrum indicated with an arrow in Fig. 3(a) at about $z = 6 \mu\text{m}$. Here, the fine structure on the high-energy side of the modes is clearly visible. If we fit the peaks by multiple Lorentzians, we receive quality factors defined by $Q = E/\Delta E$ of 2800 and 3200 for the modes at 1.186 and 1.204 eV, respectively. The origin of the signals at the high-energy side of the modes is not unambiguously clear. In our calculations so far we assumed an averaged refractive index for the microtube wall. In reality, the wall consists of multiple $\text{In}_{0.2}\text{Ga}_{0.8}\text{As}/\text{GaAs}$ bilayers. However, we have performed calculations finding that the layers are too thin and the difference in refractive index is too small to provoke further modes. In a perfect homogeneous and infinite long microtube, only light traveling perpendicular to the tube axis, i.e., having no wave vector component k_z , propagates in discrete modes. A nonzero k_z leads to spiral-shaped orbits with continuous mode energy. A finite length

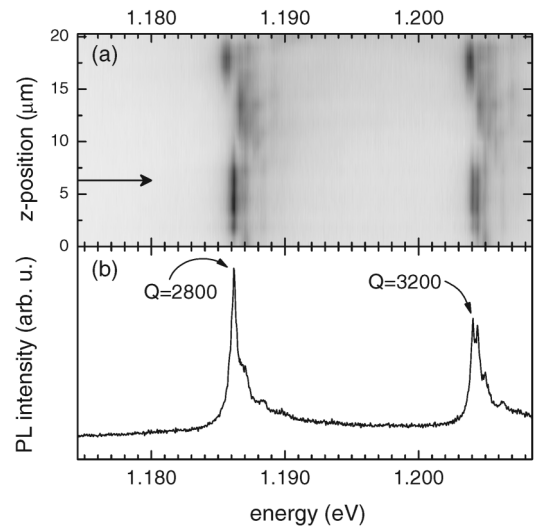


FIG. 3. (a) Gray scale plot of PL spectra measured at different positions on the microtube along its axis. Dark regions represent strong intensities. The spectrum marked with the arrow is depicted in (b).

of the microtube would allow only discrete values of k_z leading to fully discretized modes. Therefore one might interpret the strong peaks in Fig. 3 as modes with $k_z = 0$, whereas signals on their high-energy side represent modes with finite k_z . Following this model, from the fine structure of the broad signal we can approximately determine the confining length L_z in the z direction. For the spectrum depicted in Fig. 3(b) this leads to $L_z < 10 \mu\text{m}$, which is much shorter than both, the length of the whole tube ($120 \mu\text{m}$) and the length of its self-supporting part ($50 \mu\text{m}$). Interestingly, L_z is comparable to the length over which the peak positions are nearly constant [see Fig. 3(a)]. Nevertheless, until now, we cannot unambiguously prove the fine structure originating from fully confined modes with quantized $k_z > 0$.

In the following, we want to comment on the optical quality of our microtube ring resonators. Our calculation of optical modes in an ideal dielectric ring according to the exact model [21] delivers Q factors which are magnitudes higher than our measured value of about 3000. Therefore losses, like absorption, scattering, or coupling to the substrate have to be dominant. InAs QDs exhibit low absorption and therefore allow to probe higher Q factors of a cavity without masking it by internal absorption losses [2,7,22]. Scattering losses at the surface of the dielectric are the limiting factor especially in microdisks [22]. Because of the highly selective lift-off process during the preparation, the surfaces of our microtubes should be epitaxially smooth, suppressing scattering on surface roughness. However, the discontinuous radii in the region of the stricture in the tube wall will lead to some losses. Additionally, the radiative coupling of light into the neighbored substrate may decrease the Q factor. To quantify these effects, further experiments are necessary. The Q factors of state-of-the-art microcavities used in CQED experiments range from 9000 to 20 000 [5–7]. Thus, a further improvement of optical quality and a complete three-dimensional confinement of light, for example, by laterally structuring the strained bilayer before rolling, will make the novel microtube ring resonator a good candidate for CQED experiments, too.

We finally want to point out an intrinsic advantage of microtube ring resonators. Here one has the unique situation that the active material, i.e., in our case the QDs, is intrinsically located very close to the maximum optical field intensity. In the context of lasing, on the one hand this raises the quantum efficiency, since the exciting light generates carriers only inside the cavity volume, on the other hand this enhances stimulated emission similar to the situation in double heterostructure lasers, where the confinement of both, carriers and photons, leads to lower lasing thresholds compared to simple p - n laser diodes. In our microtubes, we were not able to prove stimulated emission. If we increase the pump power too much, we

burn and destroy the microtube, most likely because of a relatively poor heat flow. Nevertheless this problem should be solved by optimizing gain, losses, and heat conduction to the substrate. In the context of CQED experiments, the spacial matching of emitter and optical field is even indispensable. At least in radial and azimuthal direction, this matching is an inherent property of the microtube resonator. This is in contrast to other microcavity systems mentioned above, where usually the emitter is only in one direction, i.e., the growth direction of the sample, systematically centered in the optical field maximum.

In summary, we fabricated microtube bridges acting as ring cavities by exploiting the self-rolling mechanism of MBE-grown strained bilayers. We incorporated self-assembled InAs QDs as an internal emitter. The measured optical modes are in very good agreement to the model, where one treats the resonator as a planar dielectric waveguide with periodic boundary conditions.

We thank S. Mendach for many fruitful discussions. Financial support is acknowledged by the Deutsche Forschungsgemeinschaft via the SFB 508.

*Electronic address: tkipp@physnet.uni-hamburg.de

- [1] S. L. McCall *et al.*, Appl. Phys. Lett. **60**, 289 (1992).
- [2] J. M. Gérard *et al.*, Appl. Phys. Lett. **69**, 449 (1996).
- [3] O. Painter *et al.*, Science **284**, 1819 (1999).
- [4] K. J. Vahala, Nature (London) **424**, 839 (2003).
- [5] E. Peter *et al.*, Phys. Rev. Lett. **95**, 067401 (2005).
- [6] J. P. Reithmaier *et al.*, Nature (London) **432**, 197 (2004).
- [7] T. Yoshie *et al.*, Nature (London) **432**, 200 (2004).
- [8] V. Y. Prinz *et al.*, Physica E (Amsterdam) **6**, 828 (2000).
- [9] O. G. Schmidt and K. Eberl, Nature (London) **410**, 168 (2001).
- [10] C. Deneke *et al.*, Semicond. Sci. Technol. **17**, 1278 (2002).
- [11] M. Grundmann, Appl. Phys. Lett. **83**, 2444 (2003).
- [12] A. B. Vorobev and V. Y. Prinz, Semicond. Sci. Technol. **17**, 614 (2002).
- [13] S. Mendach *et al.*, Physica E (Amsterdam) **23**, 274 (2004).
- [14] S. Mendach *et al.*, Semicond. Sci. Technol. **20**, 402 (2005).
- [15] T. Fleischmann *et al.*, Physica E (Amsterdam) **24**, 78 (2004).
- [16] M. Hosoda *et al.*, Appl. Phys. Lett. **83**, 1017 (2003).
- [17] Y. C. Tsui and T. W. Clyne, Thin Solid Films **306**, 23 (1997).
- [18] H. Kogelnik, *Integrated Optics. Topics in Applied Physics* (Springer Verlag, Berlin, 1975), Vol. 7, Chap. 2, p. 13.
- [19] A. N. Pikhtin and A. D. Yas'kov, Sov. Phys. Semicond. **14**, 389 (1980).
- [20] T. Takagi, Jpn. J. Appl. Phys. **17**, 1813 (1978).
- [21] M. Hentschel, Ph.D. thesis, Technische Universität Dresden, 2001.
- [22] B. Gayral *et al.*, Appl. Phys. Lett. **75**, 1908 (1999).